



# Knockdown of circular RNA (CircRNA)\_001896 inhibits cervical cancer proliferation and stemness *in vivo* and *in vitro*

JIA SHAO<sup>1,2</sup>; CAN ZHANG<sup>2</sup>; YAONAN TANG<sup>2</sup>; AIQIN HE<sup>2</sup>; WEIPEI ZHU<sup>1,\*</sup>

<sup>1</sup> Department of Obstetrics and Gynecology, The Second Affiliated Hospital of Soochow University, Suzhou, 215004, China

<sup>2</sup> Department of Gynecology Oncology, Affiliated Tumor Hospital of Nantong University, Nantong, 226361, China

**Key words:** Uterine cervical neoplasms, RNA, Circular, Cell proliferation, Cancer stem cells

**Abstract: Objective:** Previous studies indicated that aberrant circular RNA (circRNA) expression affects gene expression regulatory networks, leading to the aberrant activation of tumor pathways and promoting tumor cell growth. However, the expression, clinical significance, and effects on cell propagation, invasion, and dissemination of circRNA\_001896 in cervical cancer (CC) tissues remain unclear. **Methods:** The Gene Expression Omnibus (GEO) datasets (GSE113696 and GSE102686) were used to examine differential circRNA expression in CC and adjacent tissues. The expression of circRNA\_001896 was detected in 72 CC patients using fluorescence quantitative PCR. Correlation analysis with clinical pathological features was performed through COX multivariate and univariate analysis. The effect of circRNA\_001896 downregulation on CC cell propagation was examined using the cell counting kit-8 (CCK-8) test, clonogenic, 3D sphere formation, and *in vivo* tumorigenesis assays. **Results:** Intersection of the GSE113696 and GSE102686 datasets revealed an increased expression of four circRNAs, including circRNA\_001896, in CC tissues. Fluorescence quantitative PCR confirmed circRNA\_001896 as a circular RNA. High expression of circRNA\_001896 was considerably associated with lymph node metastasis, International Federation of Gynecologists and Obstetricians (FIGO) stage, tumor diameter, and survival period in CC patients. Proportional hazards model (COX) univariate and multivariate analyses revealed that circRNA\_001896 expressions are a distinct risk factor affecting CC patients' prognosis. Cellular functional experiments showed that downregulating circRNA\_001896 substantially suppressed CC cell growth, colony formation, and 3D sphere-forming ability. *In vivo*, tumorigenesis analysis in nude mice demonstrated that downregulating circRNA\_001896 remarkably reduced the *in vivo* proliferation capacity of CC cells. **Conclusion:** CircRNA\_001896 is highly expressed in CC tissues and is substantially related to lymph node metastasis, FIGO stage, tumor size, and survival period in patients. Moreover, downregulating circRNA\_001896 significantly inhibits both *in vivo* and *in vitro* propagation of CC cells. Therefore, circRNA\_001896 might be used as a biomarker for targeted therapy in cervical cancer.

## Introduction

Cervical cancer (CC) is a prevalent gynecological malignancy, ranking fourth globally in both incidence and mortality among female cancers [1]. In developing countries, its diagnostic rate and mortality rank second and third, respectively. Notably, this cancer predominantly affects women with lower educational levels in impoverished regions [2,3]. Previous research has identified human papillomavirus (HPV) infection as a contributing factor, and despite advances in preventive vaccines and screening,

according to the World Health Organization (WHO), CC remains a significant threat to women's lives [4]. It is well known that the integration of the HPV genome into the host chromosome of cervical epithelial cells are key early events in the neoplastic progression of cervical lesions. The viral oncoproteins, mainly E6 and E7, are responsible for the initial changes in epithelial cells, which inactivate two main tumour suppressor proteins, p53, and retinoblastoma (pRb), leading to rapid cell proliferation [5]. Early-stage symptoms are often subtle, leading to delayed treatment and poorer prognosis in cases of late-stage recurrence and metastasis [6]. Exploring key molecular targets regulating cervical cancer will enhance our understanding of its pathogenesis and provide effective diagnostic markers for clinical prevention and treatment.

\*Address correspondence to: Weipei Zhu, zw3333@suda.edu.cn  
Received: 27 December 2023; Accepted: 26 February 2024;  
Published: 09 April 2024

Doi: 10.32604/biocell.2024.049092

www.techscience.com/journal/biocell



This work is licensed under a Creative Commons Attribution 4.0 International License, which permits unrestricted use, distribution, and reproduction in any medium, provided the original work is properly cited.

Studies have shown that circular RNA (circRNA) is an endogenous non-coding RNA (NCRNA), which is closed in a closed ring, without a 5' hat structure and 3' tail structure, which exists in various organisms [6,7]. One of the primary roles attributed to circRNA is its possible use as a microRNA (miRNA) sponge. It acts as a competitive miRNA binding site and regulates the synthesis of mRNA. For instance, HSA\_circRNA\_0088036 functions as a competing endogenous RNA (ceRNA) by absorbing miR-140-3P, thereby facilitating the advancement of bladder cancer [8]. CircRNA CIRCFOXK2 promotes breast cancer tumors through the insulin-like growth factor 2 mRNA binding protein 3 (IGF2BP3)/miR-370 axis [9]. Recent studies have found that circRNA plays a significant role in post-transcriptional regulation and influences the expression of its host gene during and after transcription. In addition, the abnormal circRNA expression leads to gene expression regulatory network disorders and then abnormally activates the tumor pathway, causing or promoting tumor cell growth [10]. For instance, circRNA\_100367 exhibits considerable upregulation in esophageal cancer and has a crucial impact in modulating the growth and dissemination of esophageal squamous carcinoma cells via the miR-217/Wnt3 signaling pathway [11]. Furthermore, endometrial cancer tissue exhibits higher levels of circ Wolf-Hirschhorn Syndrome Candidate 1 (circWHSC1), which promotes the migration, penetration, and propagation of endometrial cancer cells, inhibits apoptosis, and promotes the development of tumors in nude rats [12]. These findings show that the function of circRNA is crucial during tumor formation. Thus, the current study examined the differential circRNA expression in CC and its surrounding tissues via the Gene Expression Omnibus (GEO) datasets (GSE113696 and GSE102686). In CC tissues, circRNA\_001896 was found to be abundantly expressed, but its roles in CC progression have not been investigated. Therefore, we planned to further investigate the clinical importance and functions of circRNA\_001896.

## Materials and Methods

### Clinical sample collection

A total of 72 cases of CC tissue and corresponding paracancerous tissue samples from the gynecological oncology department of the hospital from August 2017 to December 2018 were collected in liquid nitrogen. All patients have confirmed CC and are included in the standard: ① The pathological diagnosis is clear; ② conforms to surgical treatment indicators; ③ No clinical treatment is undergoing before surgery; ④ Clinical data is complete and can undergo postoperative follow-up. Elimination criteria: ① merge other malignant tumors; ② serious heart, liver, and kidney insufficiency; ③ pregnancy or lactation period; ④ automatic exit during research. The exclusion criteria comprehended preoperative radiotherapy, chemotherapy, and other anti-tumor treatments. All 72 patients met the inclusion and exclusion criteria. At the same time, the patient's family members signed the consent of this study and were approved by the Second Affiliated Hospital of Soochow University Ethics Committee (No. 2022-048-54). The frozen tissue obtained is spared in liquid nitrogen.

### Fluorescence quantitative PCR (qPCR)

Cervical cancer tissues, adjacent tissues, and CC cell lines (SiHa and C33A) were extracted using the Trizol method, and concentrations were determined using Nanodrop2000 (Thermo-Scientific, Waltham, MA, USA), followed by storage at  $-80^{\circ}\text{C}$ .

In addition, to further validate circRNA\_001896, RNA was isolated from CC tissues and treated with RNase R (at  $70^{\circ}\text{C}$  for 10 min) (No. 2342, Beyotime, Beijing, China) with GAPDH serving as a positive control. The reactions were carried out using the Bio-Rad iQ5 Real Time PCR System (Invitrogen Life Technologies, Carlsbad, CA, USA), with  $\beta$ -Actin serving as the housekeeping gene. To determine the relative abundance of each gene, the double standard curve method was used. The measurement of the comparative levels of each gene was achieved via the  $2^{-\Delta\Delta\text{Ct}}$  method. Where  $\Delta\text{Ct}$  represents the Ct value of the target gene  $-\text{Ct}$  value of the reference gene, and  $\Delta\Delta\text{Ct} = \Delta\text{Ct}$  of the transfected group  $-\Delta\text{Ct}$  of the control group. The relationship between circRNA\_001896 expression and patient clinical staging, as well as prognosis, was determined by analyzing the expression levels along with patient stages and clinical records. In line with the literature [13], the primer human source sequence for circRNA\_001896 and  $\beta$ -Actin were designed by Shanghai Gima Biotech (China).

The primer for circRNA\_001896: Forward: 5'TGTGCTCCGTGAGGATGAG3'; Reverse: 5'ATCTGAAAAATCCTACGTGG3'.

The primer for  $\beta$ -Actin: Forward: 5'GTGGCCGAGGACTTTGATTG3'; Reverse: 5'CCTGTAACAACGCATCTCATATT3'.

### Cell culture and transfection

The SiHa and C33A human CC cell lines were acquired from the Shanghai Cell Bank of the Chinese Academy of Sciences. Cells were allowed to grow in Dulbecco's Modified Eagle Medium (DMEM) (No. 23423, Gibco BRL, Carlsbad, CA, USA) enriched with 10% fetal bovine serum (FBS) (No. be53340, Thermo Scientific, HyClone, Beijing China) containing 100 U/mL of penicillin and 100  $\mu\text{g}/\text{mL}$  of streptomycin (No. 23535, Harbin Pharmaceutical Group, Ltd., Harbin, China). Cell passages were performed once they entered the logarithmic growth phase. The MycAway<sup>TM</sup> Plus-Color One-Step Mycoplasma Detection Kit (No. 40612ES25, Thermo Scientific, Rockford, IL, USA) was used to examine for mycoplasma contamination, and the results were negative. Shanghai Gima Biotech developed targeting vectors for circRNA\_ knockdown (shRNA-1, shRNA-2) and a blank reference vector (shRNA-NC). Subsequently, lentiviral packaging plasmids shRNA-1, 2 and shRNA-NC were separately transfected into CC cells. The efficacy of knockdown was evaluated by using fluorescence qPCR on cells that were collected after 48 h.

### Cell counting kit-8 (CCK-8) cell proliferation assay

Cells (SiHa and C33A) under the exponential phase were seeded in a cell culture (96 well) plate, with 3 replicate wells for each experimental condition. The CCK-8 reagent (B0234, Beyotime, Beijing, China) (10  $\mu\text{L}$ ) was added at 24, 48, and 72 h subsequent to transfection using lentiviral

packaging plasmids shRNA-1, shRNA-2, and shRNA-NC. The plate was then returned to the incubator, and after 2 h, absorbance (OD) values were noted at 450 nm via a microplate reader (Bio-Tek Instruments, Thermo Scientific, Rockford, IL, USA).

#### *Clonogenic assay*

Transfected cells were grown in a culture in 6-well plate, with 600 cells per well. Media were changed every three days, and after 21 days of culture, cells were fixed for 30 min with 1 mL of 4% paraformaldehyde (32008-59-6, Merck Chemical Technology (Shanghai) Co., Ltd.). After washing with PBS three times, each well was stained with 1 mL of 1% crystal violet dye (CD434595, Guangzhou Hwei Medical Technology Co., Ltd., Guangzhou, China) for 10 min. Following another round of PBS washing, the number of colonies was counted, and this process was repeated three times.

#### *Sphere formation assay*

Transfected cells were digested, centrifuged, and resuspended into a single-cell suspension. After counting, 500 cells were added to ultra-low attachment culture dishes containing serum-free medium (20 ng/mL basic fibroblast growth factor (bFGF) (No. PHG0367, Thermo Scientific, Rockford, IL, USA), 20 ng/mL epidermal growth factor (EGF) (No. HT234, ScienCell, Carlsbad, CA, USA), and 2% B27 (No. 1537, Thermo Scientific, Rockford, IL, USA)). After 7 days of culture, the formation of cell clusters resembling spheres was observed under a microscope (CK40; Olympus Corporation, Tokyo, Japan), and results were recorded by photographing under light microscopy conditions.

#### *In vivo tumorigenicity experiment*

A total of 18 BALB/c nu/nu athymic nude female mice were purchased from the Laboratory Animal Center of Shanghai, Academy of Science Chinese (Shanghai, China). These mice were 4–6 weeks old and weighed around 18 to 20 g. Each cage contained six mice, which were acclimated in a specific pathogen-free (SPF) animal facility. Constant humidity, temperature, and a regulated light-dark cycle were provided for the care of the animals. Following acclimatization of one week, further experiments were carried out. Using the random number table method, the mice were randomly divided into three groups ( $n = 6$ ). Single-cell suspensions were prepared from healthy transfected cells, and approximately  $1 \times 10^7$  cells/mL cell density was adjusted. The dorsal area of the nude mice was cleaned with iodine, and a sterile syringe was used for injecting 100  $\mu$ L of the cell suspension into the dorsal area. All mice were maintained under a controlled environment for 30 days, with observations made every two days regarding tumor formation, food intake, water consumption, and activity. The mice were weighed regularly, and tumor dimensions were measured using calipers. The volume of the tumor (V) was determined using the formula  $V = [(a * b * b)/2]$ , where V represents the volume of the tumor, a denotes its long diameter, and b signifies its short diameter.

Additionally, body weight and tumor volume were measured for each nude mouse. At the end of the

experiment, Mice were placed in a new cage with corn cob bedding, and immediately euthanized by displacement of air with 100% carbon dioxide (124-38-9, Kedian Gas Chemical Co., Ltd., Foshan, China) for 5 min. All the experiments complied with the guidelines of the Nantong University Institutional Animal Care and Use Committee on Animal Care and Use, and were approved by Affiliated Tumor Hospital of Nantong University, Nantong Ethics Committee (No. S20240116-010).

#### *Statistical analysis*

All data were analyzed using the SPSS 20.0 software. Continuous data that followed a normal distribution was evaluated using descriptive statistics, which were expressed as mean  $\pm$  standard deviation ( $\pm$  SD). Non-normally distributed results were examined via non-parametric rank-sum tests, whereas group comparisons for normally distributed continuous data were conducted using *t*-tests or analysis of variance (ANOVA). In analyzing categorical data, chi-square tests were applied. A threshold value of  $p < 0.05$  was considered statistically significant.

## **Result**

#### *Evaluation of the level of circular RNA expression in CC tissue*

We obtained the publicly accessible circRNA expression databases GSE113696 and GSE102686 from the GEO dataset in order to assess the activity of circular RNAs (circRNAs) in CC tissues. Subsequently, using the GEO2R tool, we conducted differential expression analysis between normal cervical tissues and CC tissues. The analysis indicated that the GSE113696 database comprised 34 reduced differentially expressed genes (DEGs) and 122 elevated DEGs. In the GSE102686 dataset, there were 110 upregulated DEGs and 87 downregulated DEGs (Suppl. Table 1, Fig. 1A). Next, we constructed Venn diagrams separately for the upregulated and downregulated DEGs from the two datasets. We observed that the common upregulated genes were hsa\_circRNA\_100173, hsa\_circRNA\_001896, hsa\_circRNA\_104819, hsa\_circRNA\_104814, and the common downregulated gene was hsa\_circRNA\_100213 (Fig. 1B). In order to further explore these four circRNA\_100173, circRNA\_001896, circRNA\_104819, and circRNA\_104814, first detect the expression of the above four genes in the CC tissue and corresponding para-carcinoma tissue through the fluorescent qPCR. The expression of cancer tissue has increased substantially, of which the level of circRNA\_001896 is the most significant (Fig. 1C). Further analysis of the circRNA\_001896 sequence revealed its location on chromosome 4, spanning positions 144530863 to 144566308. It is composed of four exons, namely exons 3, 4, 5, and 6 (Fig. 1D). Therefore, in the next study, we chose circRNA\_001896 for the specific research and molecular mechanism of biological functions.

#### *Circular features identification of circRNA\_001896*

CircRNAs, in contrast to linear RNAs, are less susceptible to degradation by RNA exonucleases. Fluorescence qPCR was subsequently employed to quantify the levels of

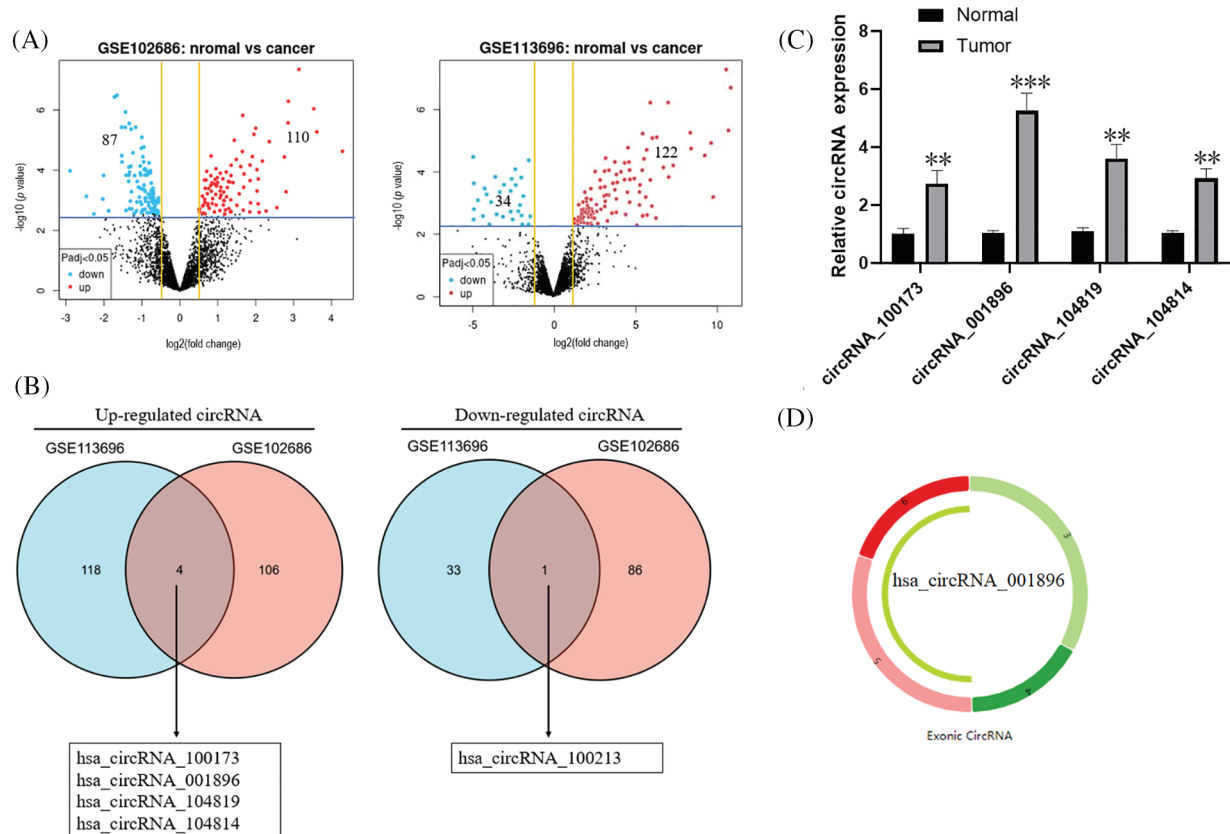


**FIGURE 1.** Analysis of the level of ring RNA in CC tissue, (A) GSE113696 and GSE102686 database mid-volcanic map display a significant difference in circular RNA, (B) Venn diagram display and screening of the circular RNA with significant differences (C) Fluorescent quantitative PCR detection circRNA\_100173, circRNA\_001896, circRNA\_104819 and circRNA\_104814 in 72 cases of CC tissue,  $n = 3$ . (D) circRNA\_001896 positioning and circularization in chromosomes, \* $p < 0.05$ , \*\* $p < 0.01$ , \*\*\* $p < 0.001$ .

circRNA\_001896 and GAPDH expression. In contrast to the placebo control, the expression of circRNA\_001896 did not change substantially by RNase R treatment. However, GAPDH expression decreased markedly following RNase R treatment ( $p < 0.01$ , showing significance differences) (Fig. 2A). This indicates that RNase R does not significantly impact the expression level of circular circRNA\_001896 but markedly degrades linear RNA (GAPDH). Additionally, divergent and convergent primers were synthesized, and PCR was performed using cDNA and genomic DNA (gDNA) as templates (cDNA obtained from reverse-transcribed mRNA and gDNA representing genomic DNA). Gel electrophoresis of the PCR products revealed that both divergent and convergent primers could amplify circRNA\_001896 fragments from the cDNA template. In gDNA, only the convergent primer could amplify circRNA\_001896, while the divergent primer did not show a distinct fragment (Fig. 2B). In the early stage of this study, 72 cases of CC tissue and corresponding para-cancerous tissue were collected, the total RNA from the tissue was isolated, and the circRNA\_001896 expressions were detected by fluorescent quantitative PCR (Fig. 2C).

According to the median expression of circRNA\_001896 in the cervical cancer tissue detected by fluorescent quantitative PCR, patients are divided into circRNA\_001896 highly expressed group and circRNA\_001896 lower expressed group to evaluate the connection between

circRNA\_001896 level and patient clinical pathological features. There is no obvious correlation between the age, organizational credentials, infiltration depth and pathological grading of cancer patients ( $p < 0.05$ ), but have a remarkable association with lymph node metastasis, FIGO staging, and tumor size. Patients are more manifested in the existence of lymph node metastasis, FIGO staging stage II, and tumor diameter 3 cm (Table 1).

#### Correlation between CirCRNA\_001896 expression and prognosis

The progression-free survival (PFS) and overall survival (OS) curves of CirCRNA\_001896 high expression group ( $N = 36$ ) and CirCRNA\_001896 low expression group ( $N = 36$ ) were constructed. The outcomes revealed that the average PFS of patients in the circRNA\_001896 lower expressed group was ( $54.18 \pm 1.86$ ) months (95% confidence interval (CI): 50.53–57.82), and the average PFS of the highly expressed group was ( $46.65 \pm 2.59$ ) months (95% CI: 41.57–51.73). circRNA\_001896 lower expressed group PFS is substantially longer than circRNA\_001896 highly expressed group ( $p = 0.039$ ). The average OS of patients with circRNA\_001896 lower expressed group is ( $57.62 \pm 1.05$ ) months (95% CI: 55.57–59.67), the average OS of the highly expressed group is ( $51.83 \pm 1.94$ ) months (95% CI: 48.03–55.63). The OS of the lower expressed group is considerably longer than the circRNA\_001896 highly expressed group ( $p = 0.035$ ) (Fig. 3).

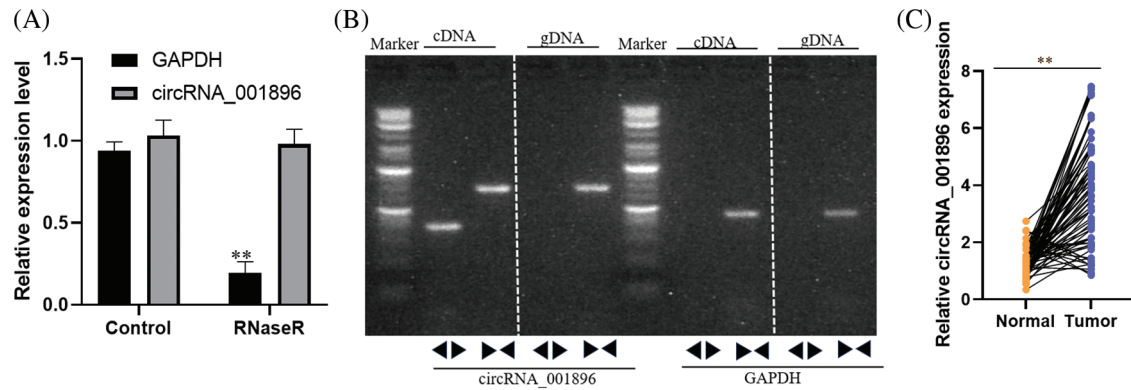


**FIGURE 2.** circRNA\_001896 positioning and ring-shaped characteristics, (A) fluorescent quantitative PCR detection circRNA\_001896 tolerances to RNase R, values are means  $\pm$  SD (n = 3 independent experiments). (B) PCR detection circRNA\_001896 back to primer (DIVERGENT PRIMER) and Converting Primer to detect cDNA and gDNA templates, values are means  $\pm$  SD (n = 3 independent experiments). (C) Fluorescent quantitative PCR was used to measure the expression of circRNA\_001896 in 72 cases of CC tissue and corresponding para-cancerous tissue. \*\* $p < 0.01$ , n = 3.

**TABLE 1**

**Analysis of the expression of circRNA\_001896 and its clinical relevance in CC patients**

Clinical features	No. of patients (n = 72)	circRNA_001896 low expression (n = 36)	circRNA_001896 high expression (n = 36)	t/ $\chi^2$	p value
Age (Years)		57.30 $\pm$ 7.25	59.17 $\pm$ 8.02	1.038	0.3029
Lymph node metastasis				6.986	0.0082
Yes	43	16	27		
No	29	20	9		
Histology				0.6435	0.4224
Adenocarcinoma	19	11	8		
Squamous cell carcinoma	53	25	28		
FIGO stage				4.431	0.0353
I	20	14	6		
II	52	22	30		
Tumor diameter				4.000	0.0455
<4 cm	24	16	8		
$\geq$ 4 cm	48	20	28		
Infiltration				2.904	0.0884
$\leq$ 1/2 Cervical stroma	27	17	10		
>1/2 Cervical stroma	45	19	26		
Pathological grading				3.603	0.0577
G1 + G2	41	24	15		
G3	31	12	19		

#### Multi-factor and single-factor assessments of the survival of CC patients using COX analysis

Combined with the patient's clinical-pathological data and the 2-year OS data for follow-up, the factors affecting the survival of CC patients were analyzed. The future prospects of CC patients are influenced by lymph node metastasis, FIGO staging, tumor size, pathological scoring, and circRNA\_001896, based on the outcome of the COX single factors ( $p < 0.05$ ) (Table 2), further COX multi-factor

analysis results. It demonstrates that pathological scoring and circRNA\_001896 level influence the prognosis of CC patients as independent risk factors ( $p < 0.05$ ) (Table 3).

#### Proliferation of CC cells in response to circRNA\_001896 knockdown

Initially, circRNA\_001896 was knocked down in CC cells with high expression. The SiHa and C33A cells were transfected with a negative control vector and knockdown vectors

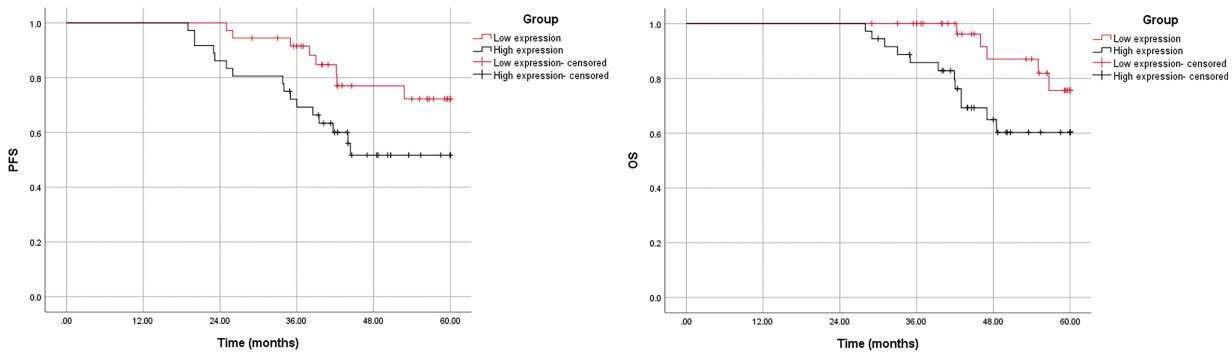


FIGURE 3. Patients with different levels of circRNA\_001896 levels with respect to PFS and OS.

TABLE 2

Affects the prognosis of CC patients with COX single factors analysis

Clinical feature	B (beta)	SE (standard error)	<i>p</i>	Exp (B)	95.0% Exp (B) CI	
					Lower limit	Upper limit
Age	-0.020	0.403	0.960	0.980	0.445	2.159
Lymph node metastasis	1.439	0.546	0.008	4.217	1.446	12.301
Histology	0.194	0.469	0.680	1.214	0.484	3.040
FIGO Stage	1.580	0.737	0.032	4.855	1.145	20.596
Tumor diameter	3.935	1.680	0.019	51.163	1.901	1376.659
Infiltration	0.795	0.469	0.090	2.215	0.883	5.556
Pathological grading	1.779	0.476	0.000	5.926	2.332	15.062
circRNA_001896 expression	0.879	0.430	0.004	5.109	1.037	13.596

Note: The B (Beta) value is the regression coefficient, indicating the strength of the influence of related factors on the results. A positive or negative B value indicates whether the factor tends to increase or decrease the risk of an event, while the absolute magnitude of the B value indicates the strength of this effect. The SE (Standard Error) value is the standard error of the B value and is used as a measure of the precision of the estimation of the B value. A smaller SE value indicates a more accurate estimate of the B value. *p* values indicate whether the result of a statistical test is significant or not. Exp (B) is the Hazard Ratio (HR), which represents the relative increase or decrease in risk by a factor.

TABLE 3

Affects the prognosis of CC patients with the prognosis of COX multi-factor analysis

Clinical feature	B	SE	<i>p</i>	Exp (B)	95.0% Exp (B) CI	
					Lower limit	Upper limit
Lymph node metastasis	0.869	0.563	0.123	2.385	0.791	7.196
FIGO stage	0.800	0.794	0.314	2.225	0.470	10.541
Tumor diameter	1.256	0.063	0.931	1.644	0.162	3.210
Pathological grading	1.166	0.544	0.032	3.210	1.105	9.320
circRNA_001896 expression	0.281	0.440	0.048	1.324	0.559	5.133

Note: The B (Beta) value is the regression coefficient, indicating the strength of the influence of related factors on the results. A positive or negative B value indicates whether the factor tends to increase or decrease the risk of an event, while the absolute magnitude of the B value indicates the strength of this effect. The SE (Standard Error) value is the standard error of the B value and is used as a measure of the precision of the estimation of the B value. A smaller SE value indicates a more accurate estimate of the B value. *p* values indicate whether the result of a statistical test is significant or not. Exp (B) is the Hazard Ratio (HR), which represents the relative increase or decrease in risk by a factor.

separately. After 48 h of transfection, the knockdown efficiency was assessed using fluorescence quantitative PCR. As opposed to the negative control group (shRNA-NC), the results revealed a substantial decrease in the level of intracellular circRNA\_001896 expressions (Fig. 4A). Subsequently, the knocked-down cell lines were seeded in a

96-well plate, and the viability of cells was assessed at 0, 24, 48, and 72 h via CCK-8 assay. The results (Fig. 4B) demonstrated that in contrast to the shRNA-NC group, shRNA-1 and shRNA-2 had no considerable impact on the propagation of CC cells at 24 h. However, a significant inhibition of cell proliferation was observed starting at 48 h

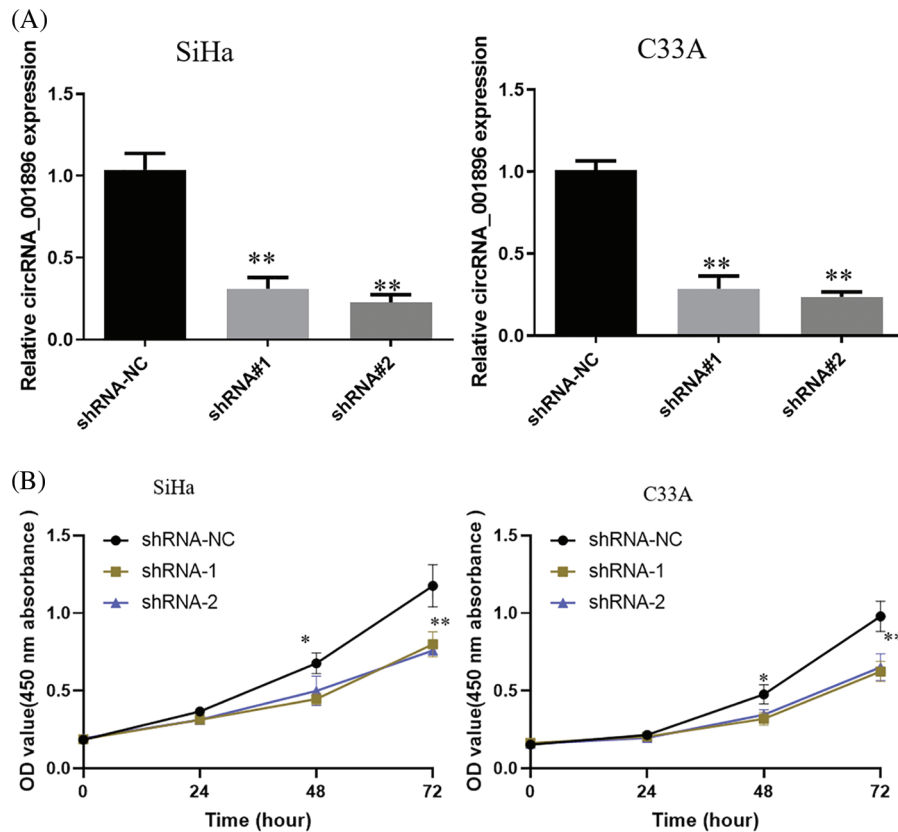


**FIGURE 4.** Impact of silencing circRNA\_001896 on CC cell growth. (A) Fluorescent quantitative PCR detects the expression of circRNA\_001896 in CC cells after transfection with interference sequences. (B) CCK-8 detects knockdown of circRNA\_001896. Impact on the proliferative ability of CC cells. Values are means  $\pm$  SD (n = 3 independent experiments). \* $p$  < 0.05, \*\* $p$  < 0.01, n = 3.

( $p$  < 0.05), and this inhibitory effect became more pronounced at 72 h ( $p$  < 0.01). These experiments suggest that circRNA\_001896 knockdown can substantially suppress the proliferative ability of CC cells (SiHa and C33A).

#### Impact of circRNA\_001896 knockdowns on CC cell clonogenic formation and stemness

Previous experimental findings suggested that circRNA\_001896 knockdowns significantly inhibited the proliferative ability of SiHa and C33A cells. Further, the

impact of circRNA\_001896 knockdowns on the ability for clonogenic formation was assessed. This was achieved by transfecting SiHa and C33A cells with knockdown vectors and a negative control vector. After 48 h of transfection, cells were seeded in a 6-well plate, fixed, stained, and photographed after 21 days of cultivation. The results (Fig. 5A) showed that, relative to the shRNA-NC group, transfection with shRNA-1 and shRNA-2 markedly suppressed the clonogenic formation of SiHa and C33A cells ( $p$  < 0.05). This suggests that circRNA\_001896 knockdowns

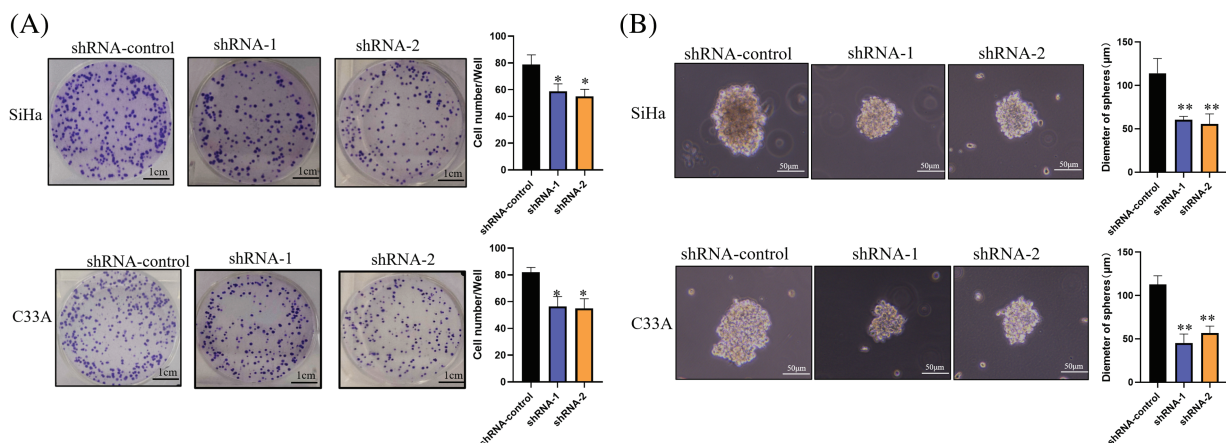


**FIGURE 5.** Impact of circRNA\_001896 knockdowns on CC cell clonogenic formation and stemness. (A) The impact of circRNA\_001896 knockdowns on the clonogenic capability of CC cells (SiHa and C33A) were illustrated via a cell colony formation experiment. (B) 3D experiment detects the impact of circRNA\_001896 knockdowns on the court ability of CC cells (SiHa and C33A). Values are means  $\pm$  SD (n = 3 independent experiments). \* $p$  < 0.05, \*\* $p$  < 0.01, n = 3.

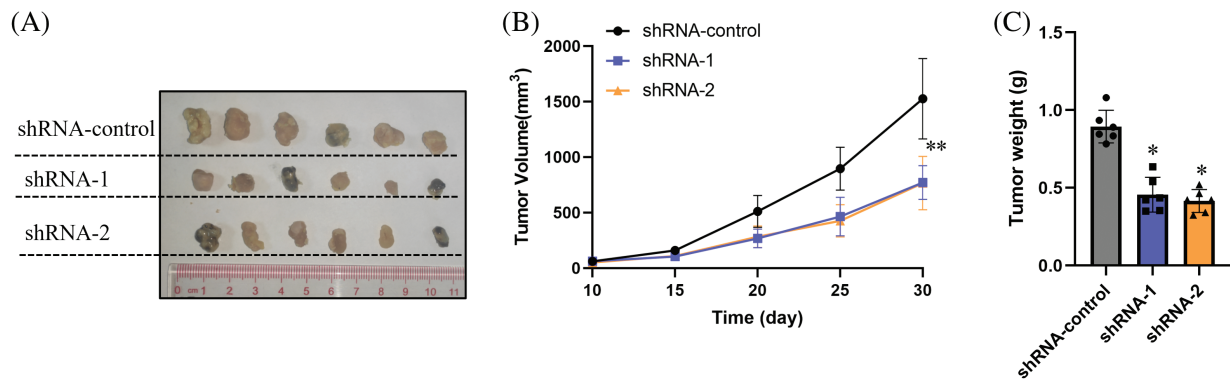


**FIGURE 6.** Impact of circRNA\_001896 knockdowns on the propagation of CC cells (SiHa) *in vivo*. (A) The morphological characteristics of the tumor-bearing tissue formed 30 days after subcutaneous inoculation. (B) The volume changes of the tumor-bearing tissue were monitored starting from the 10th day of inoculation. (C) Weight of tumor-bearing tissue formed. Values are means  $\pm$  SD (n = 6 independent experiments), \* $p$  < 0.05, \*\* $p$  < 0.01. n = 3.

significantly inhibit the clonogenic formation ability of SiHa and C33A cells.

The influence of circRNA\_001896 was further evaluated on the stemness of CC cells using 3D sphere culture; the results demonstrated that in contrast to the shRNA-NC group, transfection with shRNA-1 and shRNA-2 substantially suppressed the sphere-forming ability of CC cells. This was evident by a significant reduction in sphere diameter (Fig. 5B) ( $p$  < 0.01). This indicates that circRNA\_001896 knockdowns substantially reduced the stemness of CC cells.

#### Impact of circRNA\_001896 knockdowns on the *in vivo* proliferation capability of CC cells

To further investigate the impact of circRNA\_001896 on the *in vivo* proliferation ability of CC cells, a xenograft model was developed. Cervical cancer cells with circRNA\_001896 knockdowns were injected subcutaneously into nude mice. The measurement and observation of the dimensions (length and width) of the engrafted tumor tissue were recorded on day 10. Tumor volume was estimated by using above mentioned formula. On the 30th day, the mice were euthanized, and the engrafted tumor tissue was excised and photographed. The outcomes revealed that, in comparison to the shRNA-NC group, the volume of the tumor tissue formed by CC cells transfected with shRNA-1 and shRNA-2 was markedly reduced (Fig. 6A). Additionally, the tumor growth curve indicated a significant reduction in the volume of tumor tissue formed by cervical cancer cells transfected with shRNA-1 and shRNA-2 compared to the shRNA-NC group (Fig. 6B). Tumor tissue weight measurements further confirmed a substantial reduction in the weight of tumor tissue formed by CC cells after circRNA\_001896 knockdowns (Fig. 6C). These results suggest that circRNA\_001896 knockdowns markedly inhibit the *in vivo* propagation capability of CC cells.

#### Discussion

Cervical cancer is ranked as the fourth most prevalent form of cancer in women worldwide. Despite advances in detection and treatment methods, this gynecological malignancy continues to be highly dangerous globally, especially in

developing countries, where it poses an imminent threat to human life [14,15]. Circular RNA (circRNA) is a distinct class of endogenous non-coding RNAs, that were identified recently [16,17]. Specific expression of these molecules is observed in the eukaryotic transcriptome, where they form a covalently closed continuous loop. As understanding of circRNA has deepened, numerous studies have identified its crucial regulatory roles, especially in various diseases, including cancer [18,19].

This study reveals that high expression of circRNA\_001896 is substantially linked with lymph node metastasis, FIGO staging, tumor diameter, and survival period in CC patients. COX univariate and multivariate analyses indicate that the circRNA\_001896 level influences the prognosis of CC patients as an important risk factor. Cellular functional experiments demonstrate that knocking down circRNA\_001896 significantly inhibits CC cell proliferation, clonogenic formation, and 3D sphere-forming ability. *In vivo*, tumorigenicity experiments further show that suppressing circRNA\_001896 significantly inhibits the *in vivo* proliferative capacity of CC cells. Furthermore, studies have demonstrated an association between aberrant circRNA expression in CC tissues and the disease's pathological attributes; thus, circRNA may serve as a possible marker for early CC detection, diagnosis, personalized treatment, and survival prediction [20,21]. An increasing body of evidence suggests that circRNA participates in modulating gene expression and signaling pathways relevant to CC, influencing its occurrence and development. For instance, metastatic tissues of CC exhibit reduced levels of circ\_0005358 in comparison to *in situ* tissues. The upregulation of circ\_0005358 reduces the migration and invasion of CC cells *in vitro*, whereas the downregulation of circ\_0005358 induces the reverse effect. An intratumoral metastatic potential was found to be reduced in CC cells that overexpressed circ\_0005358 in a mouse model [22]. Circ\_0001495 further facilitates the advancement and dissemination of CC via its targeting of the miR-526b-3p/transmembrane bax inhibitor motif containing 6 (TMBIM6)/mammalian target of rapamycin (mTOR) axis [23]. Circ\_0119412 overexpression upregulates anterior gradient 2 (AGR2) expression by targeting miR-217, thereby promoting CC progression [24].

CircRNA\_101308 is downregulated in CC, acting as a tumor suppressor and participating in various processes through miRNA regulation [25]. These findings underscore the clinical research value of circRNA in the occurrence, development, and early diagnosis of CC. On the basis of the GEO database, circRNA\_001896 was initially recognized as being considerably exhibited in CC tissues in this study. In patients with CC, high circRNA\_001896 expressions were strongly associated with lymph node metastasis, FIGO stage, tumor diameter, and survival time. The level of circRNA\_001896 was identified as an independent risk factor influencing the prognosis of CC patients by univariate and multivariate analyses of COX data.

Previous work has indicated the existence of a small proportion of multipotent cells capable of self-renewal within CC tissues. These cells are frequently called cancer stem cells (CSCs) or tumor-forming cells. Tumor formation, progression, dissemination, and relapse are all considerably influenced by CSCs, making them key players in the theoretical framework of targeted CSC therapy, which aims to prevent tumor relapse and prolong patient survival [26,27]. For example, the self-renewal and differentiation of CSCs are regulated by exosomal lncRNA urothelial cancer-associated 1 (UCA1) via the microRNA-122-5p/Transcription factor SOX-2 (SOX2) axis [28]. BRM270, as an extract formulated from seven Asian medicinal plants, has been found to suppress SOX2 expression in CSCs, suppress cluster of differentiation 133 (CD133) expression *in vitro*, induce CSC apoptosis, and inhibit the proliferation and sphere-forming ability of CD133 CSCs, as well as the growth of xenograft tumors formed by SiHa and C33A cells *in vivo* [29]. Furthermore, paclitaxel resistance and CSC-like characteristics are induced by circ\_0004488 via the miR-136/mex-3 RNA binding family member C(MEX3C) axis, indicating that it may be an effective treatment option for CC [30].

By modulating the F-box protein 22 (FBXO22)/tensin homolog (PTEN) axis, ETS-like transcription factor 4 (ELK4) facilitates cell cycle development and stem cell-like features in CC associated with HPV [31]. It has been shown that CSC stemness and radiotherapy sensitivity are affected by the combination of Glycogen-synthase kinase-3 (GSK-3) and Mitogen-activated protein kinase kinase (MEK) inhibitors via regulation of the Wnt signaling pathway [32]. The current study reveals that knocking down circRNA\_001896 substantially suppresses CC cell propagation, clonogenicity, and stemness. Moreover, *in vivo* experiments further demonstrate that circRNA\_001896 knockdown restricts and inhibits the proliferative capacity of CC cells. Consequently, in the case of CC, circRNA\_001896 may function as an indicator or candidate for targeted therapy. The main effects of circRNA (non-coding RNA) involve regulating mRNA expression, competing for miRNA binding sites, and functioning as a sponge for microRNA (miRNA). Similar to mRNAs, certain circRNAs possess open reading frames (ORFs) that enable translation into peptides [33]. So there may be some possible limitations in this study: (i) the present results only showed that downregulating circRNA\_001896 reduced the *in vivo* proliferation capacity of CC cells, but the underlying mechanism(s) remains poorly

defined; (ii) we also need to construct circRNA\_001896 overexpression vector to measure the effect on CC proliferation, migration or stemness. Therefore, future experiments will continue to explore the specific regulatory mechanisms and related signaling pathways.

In conclusion, this study found a remarkable correlation between elevated levels of circRNA\_001896 and lymph node metastasis, FIGO stage, tumor size, and survival time among patients with CC. COX single-factor analysis and multi-factor analysis showed that circRNA\_001896 expression level is an important risk factor influencing the prognosis of CC patients. Cell function tests showed that knocking down circRNA\_001896 can substantially reduce the propagation, colony formation and 3D sphere formation ability of CC cells. Studies on *in vivo* tumorigenesis using nude mice demonstrated that the inhibition of circRNA\_001896 effectively impeded the expansion of CC cells. Therefore, circRNA\_001896 could potentially serve as a biomarker or therapeutic target for cervical cancer.

**Acknowledgement:** None.

**Funding Statement:** This study was supported by the Nantong Science and Technology Plan Project (No. JC2022107).

**Author Contributions:** Study conception and design: J.S; W.P.Z, data collection: C.Z; T.N.T, analysis and interpretation of results: J.S; W.P.Z; A.Q.H, draft manuscript preparation: J.S; W.P.Z; C.Z. All authors reviewed the results and approved the final version of the manuscript.

**Availability of Data and Materials:** The datasets generated during and/or analysed during the current study are available from the corresponding author on reasonable request.

**Ethics Approval:** The clinical study was approved by the Ethics Committee of the Second Affiliated Hospital of Soochow University (No. 2022-048-54) and written informed consent was obtained from each participant. All the animal experiments complied with the guidelines of the Nantong University Institutional Animal Care and Use Committee on Animal Care and Use, and were approved by Affiliated Tumor Hospital of Nantong University, Nantong Ethics Committee (No. S20240116-010).

**Conflicts of Interest:** The authors declare that they have no conflicts of interest to report regarding the present study.

**Supplementary Materials:** The supplementary material is available online at <https://doi.org/10.32604/biocell.2024.049092>.

## References

1. Wang Y, Fan PP, Feng YY, Yao XX, Peng YY, Wang RR. Clinical implication of naive and memory T cells in locally advanced cervical cancer: a proxy for tumor biology and short-term response prediction. *BIOCELL*. 2023;47(6):1365–75. doi:10.32604/biocell.2023.027201.
2. Kyrgiou M, Moscicki AB. Vaginal microbiome and cervical cancer. *Semin Cancer Biol*. 2022;86:189–98.

3. Bhattacharjee R, Das SS, Biswal SS, Nath A, Das D, Basu A, et al. Mechanistic role of HPV-associated early proteins in cervical cancer: molecular pathways and targeted therapeutic strategies. *Crit Rev Oncol Hematol*. 2022;174:103675.
4. Bedell SL, Goldstein LS, Goldstein AR, Goldstein AT. Cervical cancer screening: past, present, and future. *Sex Med Rev*. 2020;8(1):28–37.
5. Guo C, Qu X, Tang X, Song Y, Wang J, Hua K, et al. Spatiotemporally deciphering the mysterious mechanism of persistent HPV-induced malignant transition and immune remodelling from HPV-infected normal cervix, precancer to cervical cancer: integrating single-cell RNA-sequencing and spatial transcriptome. *Clin Transl Med*. 2023;13(3):e1219.
6. Narasimhamurthy M, Kafle SU. Cervical cancer in Nepal: current screening strategies and challenges. *Front Public Health*. 2022;10:980899.
7. Chen J, Gu J, Tang M, Liao Z, Tang R, Zhou L, et al. Regulation of cancer progression by circRNA and functional proteins. *J Cell Physiol*. 2022;237(1):373–88.
8. Yang J, Qi M, Fei X, Wang X, Wang K. Hsa\_circRNA\_0088036 acts as a ceRNA to promote bladder cancer progression by sponging miR-140-3p. *Cell Death Dis*. 2022;13(4):322.
9. Zhang W, Liu H, Jiang J, Yang Y, Wang W, Jia Z. CircRNA circFOXK2 facilitates oncogenesis in breast cancer via IGF2BP3/miR-370 axis. *Aging*. 2021;13(14):18978–92.
10. Kristensen LS, Jakobsen T, Hager H, Kjems J. The emerging roles of circRNAs in cancer and oncology. *Nat Rev Clin Oncol*. 2022;19(3):188–206.
11. Liu J, Xue N, Guo Y, Niu K, Gao L, Zhang S, et al. CircRNA\_100367 regulated the radiation sensitivity of esophageal squamous cell carcinomas through miR-217/Wnt3 pathway. *Aging*. 2019;11(24):12412–27.
12. Liu Y, Chen S, Zong ZH, Guan X, Zhao Y. CircRNA WHSC1 targets the miR-646/NPM1 pathway to promote the development of endometrial cancer. *J Cell Mol Med*. 2020;24(12):6898–907.
13. Mycko MP, Zurawska AE, Selmaj I, Selmaj KW. Impact of diminished expression of circRNA on multiple sclerosis pathomechanisms. *Front Immunol*. 2022;13:875994.
14. Rai R, Sehgal R, Singhal S, Suri V, Shivkumar P, Balasubramani L, et al. Cervical cancer screening coverage at tertiary care institutes across India. *Asian Pac J Cancer Prev*. 2023;24(12):4269–75.
15. Dzinamarira T, Moyo E, Dzobo M, Mbunge E, Murewanhema G. Cervical cancer in sub-Saharan Africa: an urgent call for improving accessibility and use of preventive services. *Int J Gynecol Cancer*. 2023;33(4):592–7.
16. Zhang F, Jiang J, Qian H, Yan Y, Xu W. Exosomal circRNA: emerging insights into cancer progression and clinical application potential. *J Hematol Oncol*. 2023;16(1):67.
17. Yi Q, Yue J, Liu Y, Shi H, Sun W, Feng J, et al. Recent advances of exosomal circRNAs in cancer and their potential clinical applications. *J Transl Med*. 2023;21(1):516.
18. Guan L, Hao Q, Shi F, Gao B, Wang M, Zhou X, et al. Regulation of the tumor immune microenvironment by cancer-derived circular RNAs. *Cell Death Dis*. 2023;14(2):132.
19. Jagtap U, Anderson ES, Slack FJ. The emerging value of circular noncoding RNA research in cancer diagnosis and treatment. *Cancer Res*. 2023;83(6):809–13.
20. Chen S, Yang X, Yu C, Zhou W, Xia Q, Liu Y, et al. The potential of circRNA as a novel diagnostic biomarker in cervical cancer. *J Oncol*. 2021;2021:5529486.
21. Wu M, Han Y, Gong X, Wan K, Liu Y, Zhou Y, et al. Novel insight of CircRNAs in cervical cancer: potential biomarkers and therapeutic target. *Front Med*. 2022;9:759928.
22. Cen Y, Zhu T, Zhang Y, Zhao L, Zhu J, Wang L, et al. hsa\_circ\_0005358 suppresses cervical cancer metastasis by interacting with PTBP1 protein to destabilize CDCP1 mRNA. *Mol Ther Nucleic Acids*. 2022;27:227–40.
23. Zhang X, Zheng X. Hsa\_circ\_0001495 contributes to cervical cancer progression by targeting miR-526b-3p/TMBIM6/mTOR axis. *Reprod Biol*. 2022;22(2):100648.
24. Lv Y, Wang M, Chen M, Wang D, Luo M, Zeng Q. hsa\_circ\_0119412 overexpression promotes cervical cancer progression by targeting miR-217 to upregulate anterior gradient 2. *J Clin Lab Anal*. 2022;36(4):e24236.
25. Jiao J, Jiao X, Liu Q, Qu W, Ma D, Zhang Y, et al. The regulatory role of circRNA\_101308 in cervical cancer and the prediction of its mechanism. *Cancer Manag Res*. 2020;12:4807–15.
26. Di Fiore R, Suleiman S, Drago-Ferrante R, Subbannayya Y, Pentimalli F, Giordano A, et al. Cancer stem cells and their possible implications in cervical cancer: a short review. *Int J Mol Sci*. 2022;23(9):5167.
27. Kusakabe M, Taguchi A, Tanikawa M, Wagatsuma R, Yamazaki M, Tsuchimochi S, et al. Cells with stem-like properties are associated with the development of HPV18-positive cervical cancer. *Cancer Sci*. 2023;114(3):885–95.
28. Gao Z, Wang Q, Ji M, Guo X, Li L, Su X. Exosomal lncRNA UCA1 modulates cervical cancer stem cell self-renewal and differentiation through microRNA-122-5p/SOX2 axis. *J Transl Med*. 2021;19(1):229.
29. Chandimali N, Sun HN, Park YH, Kwon T. BRM270 suppresses cervical cancer stem cell characteristics and progression by inhibiting SOX2. *In Vivo*. 2020;34(3):1085–94.
30. Yi H, Han Y, Li Q, Wang X, Xiong L, Li S. Circular RNA circ\_0004488 increases cervical cancer paclitaxel resistance via the miR-136/MEX3C signaling pathway. *J Oncol*. 2022;2022:5435333.
31. Gao F, Wang C, Bai X, Ji J, Huang X. ELK4 promotes cell cycle progression and stem cell-like characteristics in HPV-associated cervical cancer by regulating the FBXO22/PTEN Axis. *Balkan Med J*. 2023;40(6):409–14.
32. Wang C, Liu L, Cheng Y, Shi H. Combined GSK-3 $\beta$  and MEK inhibitors modulate the stemness and radiotherapy sensitivity of cervical cancer stem cells through the Wnt signaling pathway. *Chem Biol Interact*. 2023;380:110515.
33. Huang D, Zhu X, Ye S, Zhang J, Liao J, Zhang N, et al. Tumour circular RNAs elicit anti-tumour immunity by encoding cryptic peptides. *Nature*. 2024;625(7995):593–602.